Conference Proceedings

EuroSun 2016

Palma de Mallorca (Spain), 11 – 14 October 2016

Importance of thermal energy storage pilot plant facilities for solar energy applications

Gerard Peiró[1], Jaume Gasia[1], Laia Miró[1], Cristina Prieto[2] and Luisa F. Cabeza[1]

[1] GREA Innovació Concurrent, Universitat de Lleida, edifici CREA, Pere de Cabrera s/n, 25001 Lleida (Spain)

[2] Abengoa Research, C/ Energía Solar 1, 41012 Seville (Spain)

Abstract

A pilot plant facility focused on testing thermal energy storage (TES) systems both at pilot and commercial scale was designed and built at the University of Lleida in 2008. This facility was designed and equipped with the measuring devices needed to measure and analyse the thermal behaviour of all the systems tested as a previous step to commercial development. The versatility of this facility has allowed simulating real working conditions and therefore testing different TES systems, mainly for solar thermal applications such as domestic hot water, solar cooling or solar power generation, but also for other applications such as industrial waste heat recovery or combined heat and power (CHP). In this paper the main characteristics of components of the pilot plant of University of Lleida as well as the main results of the tests performed with both sensible and latent TES are shown.

Keywords: *thermal energy storage; solar thermal applications; phase change material; sensible heat; pilot plant scale*

1. Introduction

In recent years, research on renewable energies has become an important issue to achieve the main goals established by the most important international agencies and governments in order to fight against global climate change and to ensure a sustainable development for the future generations (International Energy Agency, 2014).

The most promising renewable technologies are based on solar energy. However these technologies are extremely dependent on the climate, causing temporal differences between the energy supply and the energy demand. In recent years thermal energy storage (TES) has been widely studied and represents one of the possible solutions to overcome this mismatch. Chidambaram et al. (2011) reviewed the TES systems coupled to solar cooling technologies and stated that TES integrated in solar cooling systems increases the cooling availability and improves the overall performance of the solar field. Considering solar power generation, Gil et al. (2010) showed a classification of current storage systems for solar power generation. They divided these systems depending on the materials used and the different storage concepts. They highlighted that TES systems allow a better dispatchability of power plants and enhance their power capacity.

TES systems can be classified in sensible thermal energy storage (STES), latent thermal energy storage (LTES), sorption energy storage, and thermochemical energy storage (TCES) and they can be applied in a wide range of applications at different temperatures, such as domestic hot water (DWH), solar cooling, combined heat and power (CHP), industrial waste heat (IWH) recovery, and concentrated solar power (CSP) plants. TES materials are a key factor in the solar technology field to improve the techno-economic performance. Most of the current literature evaluates the performance of the TES materials at laboratory scale (Fernandez et al. (2010); Pereira and Eames (2016)). However, it is known that the behaviour of those materials could be size-dependant (Rathgeber 2014). Moreover, there are several aspects such as operation, instrumentation, compatibility of materials (dynamic and static corrosion), and the behaviour of the TES material under the real operation conditions which need to be improved before the commercial development of the TES system. This previous research allows providing solutions to technical problems and to reduce the

Selection and/or peer review under responsibility of Scientific Committee
doi:10.18086/eurosun.2016.03.18 Available at http://proceedings.ises.org

cost of commercial plant (Rodríguez et al. (2014); Prieto et al. (2016)).

With this purpose, a pilot plant facility was designed and built at University of Lleida in 2008 (Peiró et al (2016a)). Its design simulates a real CSP plant and allows testing different sizes and configurations of TES storage tanks. Moreover, it is equipped with many measurement devices which record the different parameters to analyse the thermal behaviour of the pilot plant and their components. Up to now, this facility has been used to analyse both STES and LTES systems with configurations such as shell-and-tube tanks and two-tank system. Thus, the objective of this article is to summarize and discuss the experimentation performed using this facility.

2. Description of the pilot plant facility

The pilot plant facility presented in this paper is mainly integrated by three systems:

- The heating system, which consists of a 24 kWe electrical boiler that heats up the heat transfer fluid (HTF) simulating the solar energy source in a real application. In this facility, two different fluids have been used as HTF, thermal oil Therminol VP-1 (T-VP1) and silicone fluid Syltherm 800 (S-800). Their flow rate is measured with a differential pressure transmitter and controlled by a proportional-integral-derivative controller.
- The cooling system, which consists of an air-HTF heat exchanger of 20 kWth to cool down the HTF. It simulates the energy consumption of the real application.
- The TES system, which consists of different storage tanks that store the thermal energy during the charging process and releases it during the discharging process. These tanks are equipped with several Pt-100 temperature sensors located strategically in order to obtain a proper map of temperatures of both the TES material and HTF.

Moreover, this facility has several auxiliary systems in order to ensure a proper operation, such as pumps, piping, valves, electrical system, and control and recording data system. All these components are suitably insulated to minimise the heat losses to the surroundings. Rockwool is used for the surfaces in contact with the ambient and Foamglass and refractory concrete for the surfaces in contact with the ground. Fig. 1 shows an overview of the different components of the previously described pilot plant facility.

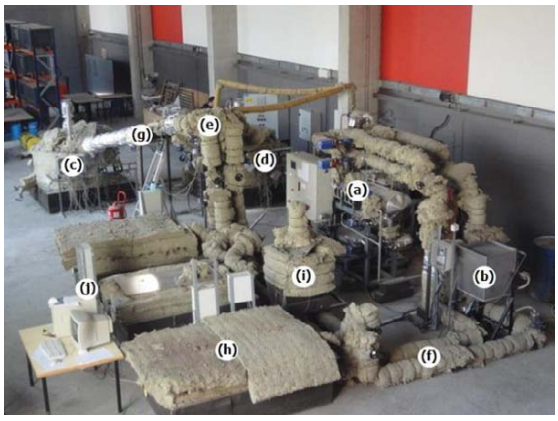

Fig. 1: Overview of the pilot plant facility available at the University of Lleida. (a) Electrical heater, (b) air-HTF heat exchanger, (c) molten salts hot tank, (d) molten salts cold tank, (e) HTF-molten salts heat exchanger, (f) HTF loop, (g) molten salts loop, (h) LTES system, (i) solid STES system, and (j) acquisition and recording system (Peiró et al. (2016a)).

3. Description of thermal energy storage systems

Different TES tanks and materials for both STES and LTES have been tested in this facility. The main characteristics of these systems are shown in this section.

3.1. Sensible thermal energy storage (STES) systems

Two different STES configurations were constructed and tested: a shell-and-tube STES tank and a two-tank TES system.

The shell-and-tube STES tank design consists of a vertical tube bundle with four tubes through which the HTF is circulated and a housing surrounding the tubes serves as storage material container. Fig. 2 shows a 3D view of the STES tank and Table 1 its design characteristics.

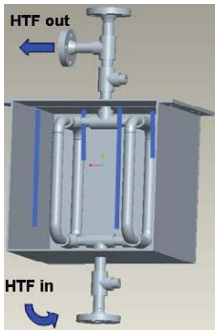

Fig. 2: Shell and tube STES tank: 3D view.

Table 1. Design characteristics of STES tank.

Dimensions of the tank	
width x height x depth	0.35 x 0.42 x 0.35 m
Packing factor	0.54
Walls of the tank	
Material	Stainless steel 304L
Thickness	0.005 m
Tubes	
Material	Stainless steel 304L
Outer diameter (OD)	0.025 m
Total length	1.74 m

The two-tank STES system is composed of two identical storage tanks (called hot and cold tanks due to their thermal level). Both tanks are designed with the same aspect ratio (L/D) than commercial storage tanks. The design of the tank consists of a cylinder-shaped vessel, where the TES material is housed, which is closed with a Klöpper cover welded on the top. Fig. 3 shows a view of the storage tank of the two-tank molten salts TES system and Table 2 its main design characteristics. The walls and cover of the tank are manufactured with some openings in order to place the electrical heaters used to heat up the TES material, to place the different measuring devices, and to place the molten salts pumps. These pumps are responsible to move the molten salts from one tank to the other tank through a multiple pass plate heat exchanger. The heat exchanger is the component responsible to carry out the heat exchange between the molten salts and the HTF (Fig. 4 and Table 3).

Fig. 3: Two-tank molten TES system.

Table 2. Design characteristics of storage tank of the two-tank molten salts TES system.

Dimensions of the tank	
Internal diameter	1.2 m
Cylinder height	0.5 m
Klöpper cover height	0.267 m
Aspect ratio	0.41
Walls of the tank	
Material	Stainless steel 316L
Thickness	0.004 m

Fig. 4: HTF-molten salts plate heat exchanger.

Table 3. Design characteristics of the HTF-molten salts plate heat exchanger.

Plate Heat exchanger	
Length x width x height	0.208 x 0.191 x 0.618 m
Plate material	Stainless steel 316

3.2. Latent thermal energy storage (LTES) systems

Two storage tanks were designed and built in order to test the LTES concept with different phase change materials (PCM). The design of the tanks was based on the shell-and-tube heat exchanger concept. It consists of a rectangular-shaped vessel with a tubes bundle inside. The PCM was located in the housing of the shell part. The HTF circulated inside the bundle of tubes, which was integrated by 49 tubes bended in U-shape and distributed in square pitch (Fig. 5). One of these tanks was built with a 196 transversal squared fins assembled along of the tube bundle in order to enhance the heat transfer between HTF and PCM (Fig. 6). Table 4 shows the main design characteristics of the LTES tanks.

Fig. 5: Shell-and-tube LTES tank without fins.

Fig. 6: Shell-and-tube LTES tank with fins.

Table 4. Design characteristics of LTES tank with and without fins.

Dimensions of the tank	
width x height x depth	0.527 x 0.273 x 1.273 m
Packing factor	0.80-0.84
Walls of the tank	
Material	Stainless steel 304L
Thickness	0.004 m
Tubes	
Material	Stainless steel 304L
OD	0.017 m
Average length	2.485 m
Tank with Fins	
Packing factor	0.80
Material	Stainless steel 304L
Number of fins	196
Dimensions	0.25 x 0.25 m
Thickness	0.0005 m

4. Description of the storage materials

A total of six different TES materials have been studied at pilot plant scale for both STES and LTES systems. Regarding the STES, two different TES materials were tested: on one hand, granulated NaCl, a by-product from the potash industry, which was used in the STES tank; on the other hand, molten salts, which were used in the two-tank system. Regarding the LTES tanks, four PCMs have been used: RT58 (a paraffin), bischofite (a by-product from the mining industry), d-mannitol (a sugar alcohol), and hydroquinone (an aromatic compound). Table 5 shows the main characteristics of these PCMs, such as specific heat for materials used in STES and melting temperature and enthalpy for materials used in LTES tank. These characteristics were obtained with differential scanning calorimeter (DSC) tests.

Table 5. Main characteristics of the STES and LTES materials used for testing.

TES Material	Type of energy storage	Specific heat [kJ/kg·K]	Melting temperature [ºC]	Melting enthalpy [kJ/kg]
NaCl	Sensible	0.738 (solid)	-	-
Molten salts	Sensible	1.51 (liquid)	-	-
RT-58	Latent	-	53-59	120.0
Bischofite	Latent	-	100-110	115.0
d-mannitol	Latent	-	162-170	246.8
Hydroquinone	Latent	-	168-173	205.8

5. Experimental procedure

Based on the operation performance of TES material, the experimentation carried out at the pilot plant facility consisted of several charging and discharging processes. Different HTF flow rates and arrangements, and different temperature ranges were considered in order to simulate real application operation conditions. In the LTES and the STES tanks the experimentation procedure is the following: before starting the charging process a warming period is done in order to achieve the initial required conditions. Once the TES material reached the initial required temperature, the HTF is heated up outside the tank until charging temperature is reached. After that, the charging process is able to start. During the charging process, the inlet temperature of HTF is kept at desired temperature. The charging process is stopped when the average temperature of the main temperature probes of the TES material tanks reaches the same temperature than the inlet HTF temperature. Then, the HTF is cooled down outside the tank with cooling system until the discharging temperature is reached. After that, the discharging process starts and it is considered finished following the same criteria than in the charging process. In the two-tank molten salts system, the charging and discharging processes are carried out with a different procedure simulating the operation in a solar power plant. During the charging process, the molten salts are pumped from the cold tank to the hot tank through the heat exchanger system. In this system, the molten salts are heated up with the HTF, which has been previously heated with the heating system. The process is considered to be finished when the level of the molten salts at the cold tank reaches the minimum level for a proper performance of the molten salts pump. On the contrary, during the discharging process, the molten salts are pumped from the hot tank to the cold tank through heat exchange system. In this system, the HTF is heated up with the molten salts to be further cooled down at the cooling system, simulating the power block. The discharging process is considered to be finished when the level of the molten salts at the hot tank reaches the lowest level.

Table 6 shows a summary of the main working conditions of the different experiments carried out at the pilot plant facility. The temperature range was selected according to the materials characteristics and to the final application, while the flow rate was selected to study its influence on the charging and discharging processes.

Table 6. Summary of the characteristics of experimentation carried out at pilot plant facility.

System	TES material	Mass tested [kg]	HTF	HTF flow rate [l/h]	Temperature range [ºC]	Ref.
STES tank	NaCl NaCl + water	59	T-VP1	1000- 3000	100-200	Miró et al. (2014)
Two-tanks	Molten salts	1600	T-VP1	435	298-343 303-372	Peiró et al. (2016b)
LTES Tank without fins	RT58	107.5	S-800	550- 2750	48-68	Gasia et al. (2016)
	Bischofite	204	S-800	1650	80-120	Gasia et al. (2015)
	Hydroquinone	170	T-VP1	500-3000	145-187 130-200	Gil et al. (2013a)
	d-mannitol	165	T-VP1	500-3000	145-187 130-200	Gil et al. (2013a)
LTES Tank with fins	RT58	106	S-800	550- 2750	48-68	Gasia et al. (2016)
	Hydroquinone	155	T-VP1	500-3000	145-187 130-200	Gil et al. (2013b) Gil et al. (2014)
Multiple PCM	Hydroquinone + d-mannitol	170 + 165	T-VP1	3000	145-187	Peiro et al. (2015)

6. Results

6.1. Sensible thermal energy storage systems

The experimental work with STES tank presented in Miró et al. (2014) was focused on comparing the thermal behaviour of granulated NaCl and NaCl compacted with water. Four thermal cycles (charge and discharge) were performed with temperature range of 100-200 ºC. The main differences between the thermal cycles were the HTF flow rate (1000 l/h and 3000 l/h) and the duration of the processes (4 h and 8 h).

Fig. 7a and Fig. 7b show the temperature profile of the HTF and average temperature of both granulated NaCl (salt A) and NaCl compacted with water (salt B). In the four thermal cycles performed, both salt A and salt B do not reach the fixed temperature set-point for charging (200 ºC) because the two proposed intervals of time were not sufficient to ensure a full charge. However, it can be observed that the temperature profile of the salt A and salt B are significantly different. Notice that at the end of the 4 h charging process (Fig. 7a) the salt B temperature is around 25 ºC higher than the temperature of salt B. The reason lies on the fact that the thermal conductivity of salt B (2.84 W/m·K) is 8.6 times higher than the salt A (0.33 W/m·K). From Fig. 7a, it also can be observed that there are not significant differences between the temperature profiles of the salts when the HTF flow rate was increased. Moreover, during this experimentation the energy accumulated or delivered by the salts was analyzed. During the charging process, salt A average accumulated energy was 0.63 kWh, while it was 0.75 kWh for salt B (the wetted compacted salt). This fact represented an increase of 19% in energy accumulated when using salt B. During the discharging process the average energy delivered by salt A was 0.40 kWh and 0.66 kWh for salt B. That represented an increase of 68%. The reason is because in the same period of time, the conductivity had a big impact. The average thermal efficiency was 63% for salt A and 88% for salt B, which represented an increase of 40%. It was also observed that there was no influence in the energy accumulated with an increase of the HTF flow rate. As expected, when the duration of experiments was doubled, an average increase of 27.8% (salt A) and 16.3% (salt B) of the energy accumulated during the charging process, and an increase of 30.6% (salt A) and 22.3% (salt B) of the energy delivered during the discharging process. With these results, the main conclusion reported in the study performed by Miró et al. (2014) is that NaCl compacted with water represents a better and cheaper option than other STES materials for TES due to the reduction of air gaps inside the solid.

The two-tank molten salts TES system experimentation presented in Peiró et al (2016) represents the first study in the literature at pilot plant scale with molten salts as TES material and thermal oil (Therminol VP-1) as HTF operating in a plate heat exchanger. The main objective of this work was to study the effects of varying the flow arrangement (parallel and counter flow) in the plate heat exchanger and the effects of modifying the temperature gradient between the HTF and the molten salts (46 ºC ± 3 ºC and 68 ºC ± 1 ºC).

From the results of the experiments carried out, it was observed that for the same temperature gradient, counter flow arrangement performed better than parallel flow. Higher values of power were obtained with counter flow arrangement in both charging and discharging processes (from 65.5% to 78.8% higher). The reason of this behavior lies on the fact that in counter flow arrangement a more constant thermal gradient between the hot and the cold fluid at the heat exchanger is obtained during the whole process. On the other hand, it was observed that with the same flow, the experiments carried out with a higher thermal gradient provided values of power from 12.9% to 35.5% higher in both charging and discharging processes as a result of an increase in the driving force for the heat transfer.

Fig. 7c and Fig. 7d show the temperature evolution of both HTF and molten salts during the charging and discharging processes at inlet and outlet of the heat exchanger of two-tank system for the best working conditions (counter flow arrangement with a temperature gradient between 305 ºC and 370 ºC). The shaded areas represent the periods used to achieve the operational conditions required for the experimentation. The HTF temperature is represented in dotted lines while the molten salts are represented in straight lines. Moreover, in both charging and discharging processes, the hot fluids are plotted in red while the cold fluids are plotted in blue. During the charging process (Fig. 7c), the energy released by the HTF (7.8 kWh with an average thermal power of 13.0 kW) is higher than the energy absorbed by the molten salts (6.8 kWh with an average thermal power of 11.6 kW), which gives a process efficiency of 89%. On the contrary, during the discharging process (Fig. 7d), the energy released by the molten salts (7.5 kWh with an average thermal

power of 11.75 kW) is higher than the energy absorbed by the HTF (7.09 kWh with an average thermal power of 11.12 kW), which gives a process efficiency of 94.53%. The differences between the energy of HTF and salts are due to the heat losses of heat exchanger. Notice that the energy released by the salts during the discharge is higher than the energy absorbed in the charge process, due to the salts temperature difference between the inlet and outlet, which is slightly higher in discharge than in charge as a result of the electrical resistances placed inside the hot storage tank.

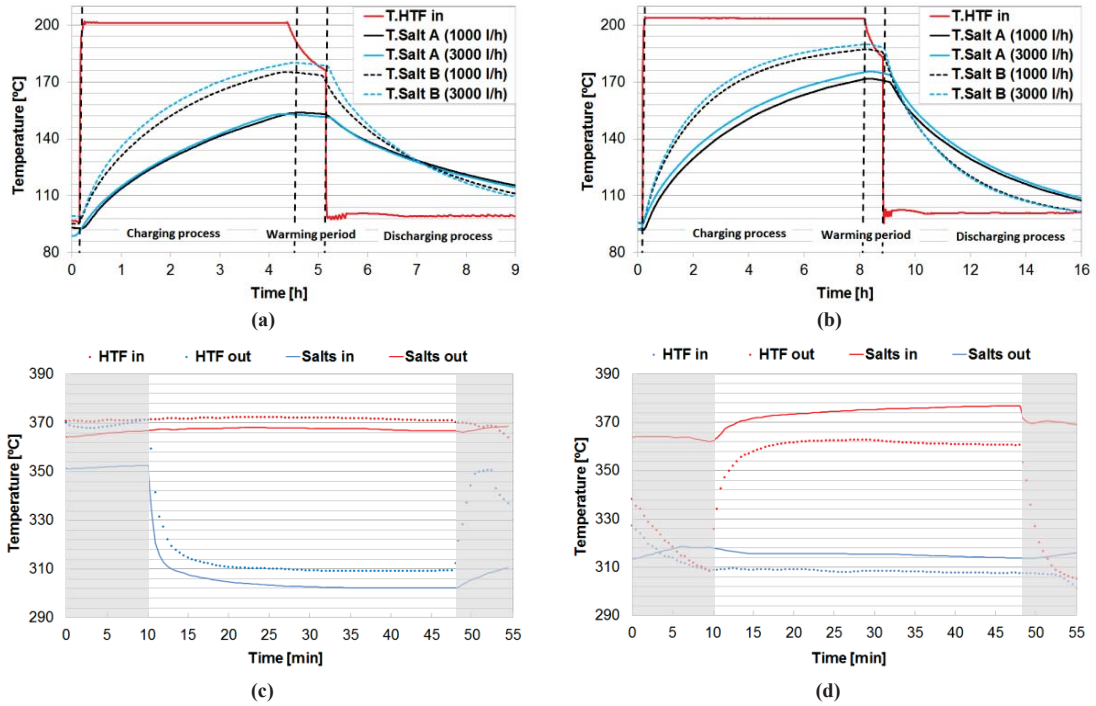

Fig. 7: STES systems temperature profiles. STES system: (a) thermal cycle of 4h and (b) thermal cycle of 8h. Two-tank molten salts TES system: (c) charging process and (d) discharging process.

6.2. Latent Thermal Energy Storage systems

The LTES systems, with the four above-mentioned PCMs, were analyzed under different HTF flow rates and working temperatures in order to test different operational conditions. Moreover, the effect of adding extended surfaces and the arrangement in series of different PCM's with different melting temperature and melting enthalpies were also studied.

The first PCM presented in this paper is RT58. This material was selected for DWH taking into account its melting temperature range (Table 5). The experimental work with RT58 presented in Gasia et al. (2016) was carried out with the objective of characterizing this material as PCM. Several charging and discharging processes were performed with a temperature range of 48-68 ºC for three different flow rates: 550 l/h, 1650 l/h and 2750 l/h. Fig. 8a shows the HTF and average temperature of RT58 charge and discharge temperature profiles for the different HTF flow rates. Notice that the higher the flow rates, the faster the PCM was charged or discharged. Taking into account the properties of Sylthem 800, only laminar flow regime could be achieved. Hence, the heat transfer coefficient was constant for the different flow rates evaluated, and therefore the temperature difference between HTF and PCM determined the value of heat transfer rate. With a higher flow rate, the temperature difference was higher and, as a consequence, the heat transfer was higher, which caused the PCM to heat up or cool down faster. The energy accumulated and delivered by the HTF and RT58 was also analysed. For instance, during the charging process with an HTF flow rate of 1650 l/h, the energy stored by the PCM was 5.74 kWh and the energy released by the HTF was 6.33 kWh, giving an efficiency of 90.68%. During the discharging process, the energy recovered by the HTF was 5.03 kWh, which was obtained from the PCM and the metallic parts of the TES system, which gives an efficiency of 89.15 %.

Regarding the evaluation of bischofite, Gasia et al. (2015) studied the suitability of bischofite as TES material in both sensible storage and latent storage. This material was selected for IWH and CHP purposes taking into account its melting range of temperatures (100-110 ºC). Several charging and discharging processes with a flow rate of 1650 l/h were performed, going from from 50 ºC to 80 ºC to evaluate the TEs material under the sensible form, and from 80 ºC to 120 ºC to test the latent form (Fig. 8b). Notice that the first two hours corresponded to the charge in sensible form, and from the 3rd hour until 7.64 h corresponded to the latent form. Discharging took place between 9.69 h and 14.12 h. During the experimentation, the subcooling effect at pilot plant scale was observed to be lower than the results obtained at laboratory scale. Regarding in energy stored/released during the first charging process, it was observed that the energy released by the HTF was 4.02 kWh and the energy stored by the bischofite was 3.07 kWh, giving an efficiency of 76.4%. During the second charging process, the energy given by the HTF was 13.5 kWh and the energy stored by the bischofite was 11.97 kWh, giving an efficiency of 88.7%. The reason for this difference between the two charging processes lies on the fact that while in the first charging process the bischofite increased 30 ºC in the sensible form, in the second charging process the bischofite increased 40 ºC in both the sensible and latent form. Moreover, results showed a good behavior of the 204 kg of bischofite evaluated at pilot plant but further research is needed because of the bischofite nature and the impurities embedded in it.

As shown in Table 6 two more PCMs have been studied, tested and compared at the pilot plant of University of Lleida in order to find the best PCM candidate for a real solar cooling plant available at University of Seville (Spain)(Gil et al. (2013a)). Several charging and discharging processes were performed with two different temperature ranges, 130-200 ºC and 145-187 ºC, and with three different flow rates: 1400 l/h, 2200 l/h and 3000 l/h (Fig. 8 c and Fig. 8d). As for the results obtained with RT58, the higher the flow rates, the faster the PCMs were charged or discharged. However, due to the thermophysical properties of the Therminol VP-1, the three representative flow regimes could be obtained for the three studied flow rates: laminar, transition and turbulent. The subcooling effect at pilot plant scale of hydroquinone was also lower than the results obtained at laboratory scale. However, d-mannitol showed high subcooling and polymorphism at pilot plant scale. Furthermore, for the same boundary conditions, the energy stored and released by d-mannitol was higher than hydroquinone. For instance, during the charging process with d-mannitol as PCM, with a temperature range of 145-187 ºC and an HTF flow rate of 1400 l/h, the energy released by the HTF was 22.35 kWh and the energy stored by the d-mannitol was 19.89 kWh, giving an efficiency of 88.9%. On the other hand, with hydroquinone, the energy released by HTF was 17.55 kWh and the energy stored by hydroquinone was 14.82 kWh, giving an efficiency of 84.4%. During the discharging process with d-mannitol, the energy recovered by the HTF was 18.11 kWh and energy released by d-mannitol was 18.46 kWh, giving an efficiency of 88.6 %. With hydroquinone, the energy recovered by the HTF was 13.30 kWh and the energy released by hydroquinone was 14 kWh, giving an efficiency of 92%. Results showed that d-mannitol and hydroquinone were good candidates as PCM for solar cooling applications. However, the subcooling effect is a parameter which should be addressed if these materials are selected.

In all the PCMs evaluated, it was found that that one of the most important drawbacks were their low values of thermal conductivity in both solid and liquid, which causes a limitation in the heat transfer ratios between the HTF and the PCM. In order to overcome such drawback, different heat transfer enhancement techniques were tested at the pilot plant facility. Two studies were carried out with the aim of evaluating the influence of adding fins: hydroquinone (Gil et al. 2013b) and RT58 (Gasia et al 2016). Another project was carried out with the objective of testing the multiple PCM concept, or cascaded, with hydroquinone and d-mannitol (Peiró et al 2015). Results showed that the addition of fins increased up to 28% the time of the charging/discharging process under the same working conditions. Moreover, results also showed that the multiple PCM configuration introduced a higher uniformity on the HTF temperature, and introduced an effectiveness enhancement of around 20%.

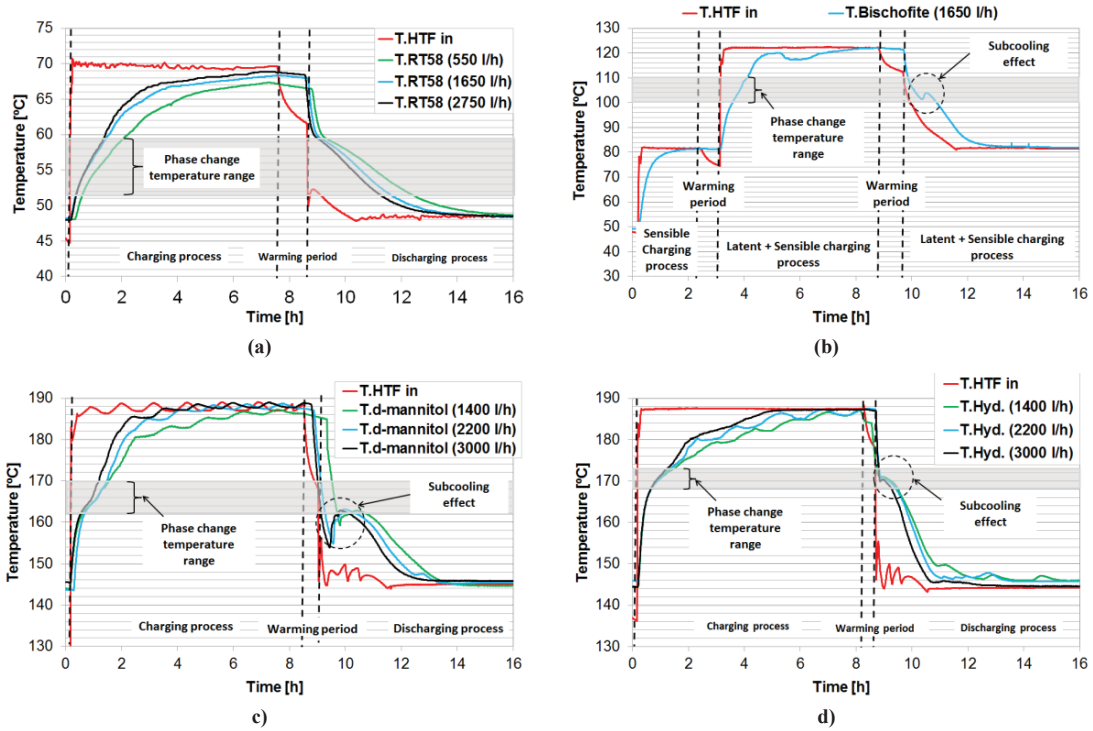

Fig. 8: Charge and discharge LTES tank temperature profiles of HTF and PCM. a) RT58 b) bischofite. c) d-mannitol and d) hydroquinone.

7. Conclusions

In the literature, most of the TES materials thermal behaviour analyses are performed at laboratory scale. Taking into account that some thermophysical properties are present size-dependant behaviour, analyses at higher scales are needed.

In the present paper, some results of all the experimentation performed at the pilot plant facility designed and built at University of Lleida with different TES materials (in both sensible and latent forms) are presented. In the experimentation carried out to test STES materials, a TES tank based on shell-and-tube heat exchanger concept and a two-tank molten salts system were used. In the experimentation performed to test LTES materials, a different storage tank based on shell-and-tube heat exchanger concept. The effects of the TES materials thermophysical properties, HTF flow rates, the addition of fins, and the multiple PCM concept was tested and analysed. Moreover, six different materials were used in the experimentation: NaCl and molten salts as STES materials, and RT-58, Bischofite, d-mannitol and hydroquinone as PCM.

The experimentation carried out at the pilot plant facility of the University of Lleida, has shown the relevance of testing at a relevant scale in order to face important progress in the roadmap to reach commercial development. A proper design of a pilot plant has allowed the evaluation of various materials, different designs of TES tanks, instrumentation, auxiliary equipment, and different operational strategies such as the effect of adding fins or the flow arrangement, using the same installation. Moreover, this experimentation has shown that the thermophysical behaviour of the TES materials is different at different scales such as subcooling effect.

Acknowledgements

The research leading to these results has received funding from Spanish goverment (Fondo tecnológico IDI-20090393, ConSOLida CENIT 2008-1005) and from Abengoa Solar NT. The work is partially funded by the Spanish government (ENE2008-06687-C02-01/CON, ENE2011-22722, ENE2015-64117-C5-1-R (MINECO/FEDER) and ULLE10-4E-1305). The authors would like to thank the Catalan Government for the quality accreditation given to their research group GREA (2014 SGR 123). This project has also received

funding from the European Commission Seventh Framework Programme (FP/2007-2013) under Grant agreement NºPIRSES-GA-2013-610692 (INNOSTORAGE) and from the European Union's Horizon 2020 research and innovation programme under grant agreement No 657466 (INPATH-TES). Laia Miró would like to thank the Spanish Government for her research fellowship (BES-2012-051861). Jaume Gasia would like to thank the Departament d'Universitats, Recerca i Societat de la Informació de la Generalitat de Catalunya for his research fellowship (2016FI_B 00047).The authors would like to thank Dr. Eduard Oró from Catalonia Institute for Energy Research (Spain) and Dr. Antoni Gil from Massachusetts Institute of Technology (USA) for their help during the initial stages of the experimentation.

References

Chidambaram, L.A., Ramana, A.S., Kamaraj, G., Velraj, R., 2011. Review of solar cooling methods and thermal storage options. Renew. Sust. Energ. Rev 15, 3220-3228.

Fernandez, A.I., Martinez, M., Segarra, M., Martorell, I., Cabeza, L.F., 2010. Selection of materials with potential in sensible thermal energy storage. Solar Energy Materials & Solar Cells 94, 1723-1729).

Gasia, J., Gutierrez, A., Peiró, G., Miró, L., Grageda, M., Ushak, S., Cabeza, L.F., 2015. Thermal performance evaluation of bischofite at pilot plant scale. Appl.Energ. 155, 826-833.

Gasia, J., Miró, L., de Gracia, A., Barreneche, C., Cabeza, L.F., 2016. Experimental evaluation of a paraffin as phase change material for thermal energy storage in laboratory equipment and in a shell-and-tube heat exchanger. Appl. Sci. 6(4), 112.

Gil, A., Medrano, M., Martorell, I., Lázaro, A., Dolado, P., Zalba, B., Cabeza, L.F., 2010. State of the art on high temperature thermal energy storage for power generation. Part 1—Concepts, materials and modellization. Renew. Sust. Energ. Rev. 14, 31–55.

Gil, A., Oró E., Peiró, G., Álvarez, S., Cabeza, L.F. 2013a. Material selection and testing for thermal energy storage system in solar cooling. Renew. Energ. 57, 3661-371.

Gil, A., Oró, E., Castell, A., Cabeza, L.F., 2013b. Experimental analysis of the effectiveness of a high temperature thermal storage tank for solar cooling application. Applied Thermal Engineering 54, 521-527.

International Energy Agency https://www.iea.org/ [accessed: 29/08/2016].

Miró, L., Navarro, M.E., Suresh, P., Gil, A., Fernández, A.I., Cabeza, L.F., 2014. Experimental characterization for a solid industrial by-product as material for high temperature sensible thermal energy storage (TES). Appl.Energ. 113, 1261-1268.

Peiró, G., Gasia, J., Miró, L:, Cabeza, L.F., 2015. Experimental evaluation at pilot plant scale of multiple PCMs (cascaded) vs. single PCM configuration for thermal energy storage, Renew. Energy 83, 729-736

Peiró, G., Prieto, C., Gasia, J., Miró, L., Cabeza, L.F., 2016 a. Two-tank molten salts thermal energy storage system for solar power plants at pilot plant scale: lessons learnt and recommendations for its design, start-up and operation. Submitted to Sol Energy.

Peiró, G., Gasia, J., Miró, L., Prieto, C., Cabeza, L.F., 2016b. Experimental analysis of charging and discharging processes, with parallel and counter flow arrangements, in a molten salts high temperature pilot plant scale setup. Appl. Energy 178, 394-403.

Pereira da Cunha, J., Eames, P., 2016. Thermal energy storage for low and medium temperature applications using phase change materials – A review. Appl. Energy 177, 227-238.

Prieto, C., Osuna, R., Fernández, A.I., Cabeza, L.F., 2016. Molten salt facilities, lessons learnt at pilot plant scale to guarantee commercial plants; Heat losses evaluation and correction. Renew. Energ. 94, 175-185.

Rathgeber, C., Miro, L., Cabeza, L.F., Hieber, S. 2014. Measurement of enthalpy curves of phase change materials via DSC and T-History. When both methods needed to estimate the behaviour of the bulk materials in applications. Thermochim. Acta. 596, 79–88

Rodríguez-García, M.M., Herrador-Moreno, M., Zarza-Moya, E., 2014. Lessons learnt during the design, construction and start-up phase of a molten salt testing facility. App. Therm. Eng. 62, 520–528.